stellarator news

Published by Fusion Energy Division, Oak Ridge National Laboratory
Building 9201-2; P.O. Box 2009; Oak Ridge, TN 37831-8071, USA

Editor: James A. Rome Issue #13 January, 1991

Eighth International Workshop on Stellarators

The Eighth International Workshop on Stellarators will be a Technical Committee Meeting of the International Atomic Energy Agency and will be hosted by the Kharkov Institute of Physics and Technology and the State Committee on Atomic Energy of the USSR. The workshop will be held May 27–31, 1991 in the conference hall of the Kharkov Institute of Physics and Technology.

The workshop will cover all topics applicable to stellarators and other helical confinement devices. Topics of interest are: experimental results, theory, diagnostics of special interest to helical devices, and future devices. The number of oral presentations will be limited to emphasize overview talks, reviews of recent works, and topics of general interest. More detailed papers will be presented in poster sessions. Ample time will be set aside for free discussion.

Participation in the Workshop is limited to 120 persons. Interested persons should notify the Workshop Secretary, Dr. V. Tereshin, of their intention to attend the meeting and provide a tentative title of their presentation (and whether poster or oral presentation is preferred) by January 31, 1991. A one-page abstract of each paper is needed by March 4, 1991.

V. Tereshin
Kharkov Institute of Physics and Technology
Plasma Physics Division
Academicheskaja, 1
Kharkov 310108, USSR
Telephone: (007)-(057)-2351993, ext. 015
FAX: (007)-(057)-2352664
Telex: 115 175 DECAN SU

Around the Labs

Record high-speed pellet injector

A two-stage pneumatic pellet injector for Heliotron E, with relevance for other magnetic confinement machines, has been constructed and tested in order to provide increased pellet velocity. The increased velocity will allow more flexible control of the density profile of the Heliotron E plasma and will produce a wider range of pellet velocity for pellet ablation studies. Pellet velocity is limited to around 1.4 km/s for the present six-pellet injector on Heliotron E, which has successfully operated for several years.

The fundamental operation of the new pellet injector was simulated using the code Quickgun developed by Dr. S. Milora of ORNL. The experimental results generally agree well with the code calculations if we assume an effective diameter for the fast valve orifice. By devel-

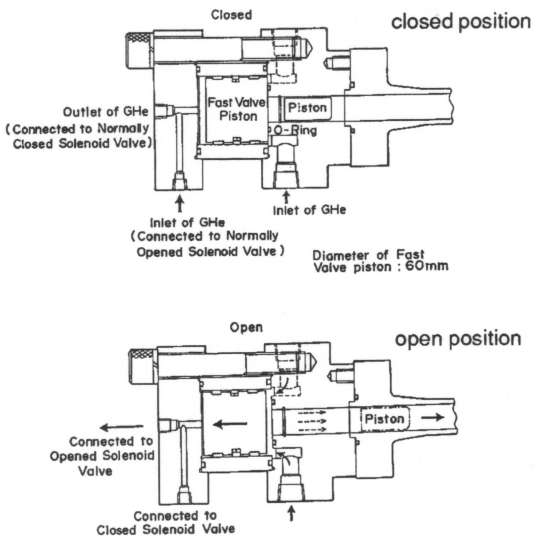

Schematic of the high-pressure fast valve

oping a high-pressure fast valve, we have achieved a hydrogen pellet velocity of 3.2 km/s without using a sabot. This is the world record for hydrogen pellets without sabots.

The high performance of this two-stage injector is partly due to a specially developed high-pressure fast valve with a very large conductance as shown in the figure. We studied the dependence of the pellet velocity and breech pressure on the pump tube fill pressure. The results show that the fill pressure is a very sensitive parameter. We also investigated the effect of the clearance between piston and pump tube wall on the pellet velocity, and the exhaustion and damage of the piston caused by the compressing propellant gas. The changes to the piston surface differ quite a lot depending on whether the fill gas is hydrogen or helium.

Shigeru Sudo
Plasma Physics Laboratory
Kyoto University
Uji, Kyoto, Japan

News from CHS

Experimental study of the field error effects on confinement has been carried out under the US/Japan collaboration program. Two error field coils mounted on the top of the CHS device with 180° separation between them in the toroidal direction can produce a vertical error field of the order of 10 G at the plasma center in the experiment with a 1-T magnetic field. Islands of $m = 2$, $n = 1$ are produced at the $q = 2$ surface, when the current directions for the two coils are opposite.

Experiments were carried out both for ECH and NBI plasmas at a magnetic axis of $R_{ax} = 100.8$ cm (outward shifted). This configuration was chosen so that the width of the $m = 2$ island becomes large, because the magnetic shear at the $q = 2$ surface is small. The stored energy measured by the diamagnetic loop was reduced by 10–20% for the NBI plasma with the perturbation coils excited. The difference in the diamagnetic loop signal is more significant for the ECH case though the noise due to magnetic field ripple is larger. The radial profiles of the electron density and temperature have been measured by Thomson scattering. The toroidal phase of the island (O-point or X-point) at the Thomson scattering chord can be changed by reversing the current direction. No clear difference between ECH and NBI plasmas was observed with the profile measurement, although we have only preliminary data. The disagreement of the two diagnostics is not yet understood. Vacuum magnetic surface mapping with the error field is planned.

A lithium pellet injector is now operational and initial testing has been carried out. Increases in line density and stored energy with an appropriately sized pellet were observed without radiation collapse. This is different from the previous hydrocarbon pellet injection experiment. The experiment will continue in January.

Special diagnostic systems have been set up for neutral hydrogen measurements. The poloidal and toroidal arrays for the H_α emission detector system are now absolutely calibrated. A laser fluorescence method is to be applied soon. Those diagnostics have progressed under a collaboration with Kyushu University. Improved understanding of particle transport is a goal of the experiment.

Harukazu Iguchi for the CHS Group
National Institute for Fusion Science
Nagoya, 464-01 Japan

Development of Kyoto negative ion source

During the past several years, the Heliotron-E NBI system has revealed a number of interesting physics issues that should be explored to find the best confinement regimes in helical systems. One recent exciting topic was concerned with magnetic configuration studies, by which a new regime of improved confinement was found using additional toroidal and vertical fields. Data analysis of these MHD/transport results is now under way.

The NBI group is now developing a next-generation NBI system which uses negative ion sources in a high-energy regime [1]. The ion source is a modified version of a circular cylindrical bucket-type positive ion source (30 cm diameter, 19 cm long), in which a magnetic filter of the rod type is housed. The filter divides the arc chamber into two regions: (I) driver volume and (II) extraction volume.

To understand the underlying atomic and molecular processes that occur in the Kyoto negative-ion source, measurements of plasma parameters were made using electrostatic probes, spectral emission lines, and a photodetachment technique.

The novel photodetachment technique was applied to measure the H^- density (n_-) in chamber II. The Nd-YAG laser (1.064 μm) of 8-mm diameter, 30-ns duration, and 30-mJ energy was used to detect the photodetachment electrons emitted from the laser-illu-

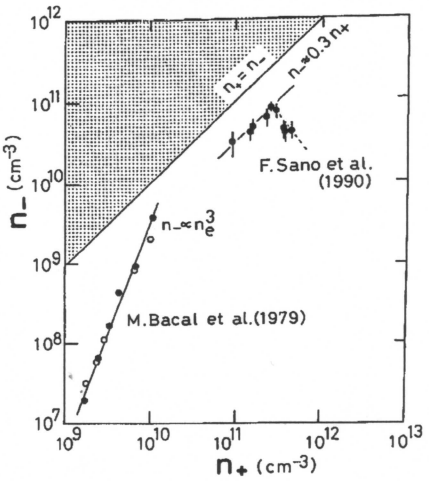

Fig. 1. H^- ion density (n_-) as a function of positive ion density (n_+). Our data are compared with Bacal's data which shows a marked difference of H^- confinement behavior.

minated region. The present laser energy is at a sufficient level for achieving the $\Delta n_-/n_-$ saturation requirement. Photodetachment signals with a different material gases (H_2, He and D_2) were compared in order to confirm the photodetachment mechanism occurring in the detection region. H^- density characteristics in chamber II, as determined by this technique, so far satisfactorily explain the behavior of the extracted negative ion current density on the beam axis. The H^- density behavior obtained here has been compared with that of the pioneering work by M. Bacal et al. [2] as shown in Fig. 1. Although Bacal's data show the relation of $n_- \propto n_e^3$, our data indicate $n_- \approx 0.3 n_+$ (or $n_- \approx 0.42 n_e$) under optimal conditions in the much higher density region.

The observed behavior clearly shows that the loss of negative ions is dominated by destruction (mutual neutralization and detachment in electron collisions) rather than by diffusion. Equilibrium rate calculations including the dominant effects of vibrationally excited hydrogen molecules ($H_2(v'' = 7\sim 10)$) also support this interpretation. This experimental result predicts $H_2(v'')$ wall bounces on the order of 10 to 40 if the wall-related $H_2(v'')$ reaction rates are small. The comparison with theory (provided by J. R. Hiskes et al. [3]) is interesting and should be done, in combination with the experimental data of $H_2(v'')$ distribution. A model predicts that the $H_2(v'')$ density $n(v'') \approx 8.4 n_+$ for our experimental conditions.

In order to estimate the H^- emission current density, the experimental determination of the H^- ion thermal velocity $\langle v_- \rangle$ in chamber II is very important. An approach to estimating $\langle v_- \rangle$ is to analyze the plasma dynamics subsequent to photodetachment. The time at which the probe current returns to zero, Δt, was assumed to correspond to the arrival of a group of slow H^- ions. Therefore, $(v_-)_{min} = (R - r)/\Delta t$, where R is the radius of the laser beam and r is the radius of the probe. A typical value of $\Delta t \sim 0.5$ μs, as shown in Fig. 2, provides $(v_-)_{min} \sim 2$ km/s, which is over a factor of 2 smaller than the theoretical $(v_-)_{min} \sim 5.2$ km/s predicted by J. M. Wadehara [4].

The characteristics of n_-/n_e as a function of arc current showed that the ratio n_-/n_e increased with an increase in source pressure at high arc currents. However, with D_2 operation n_-/n_e was a factor $3 \sim 4$ lower than with H_2 operation. The reason is not yet clear, and now related studies are under way.

Application of a positive bias voltage between the arc chamber and the plasma grid enhanced the ratio of n_-/n_e up to ≈ 1, which means that half of the negative charges in chamber II were ascribed to H^- (!).

With the progress of grid conditioning, a factor OF 2 increase in acceleration voltage (13–27 kV) recently resulted in a remarkable increase of the extracted $H^0 + H^-$ current density (calorimeter detected $H^0 + H^-$ current/9-hole area). At present, an arc current of more than 400 A at 27 kV can provide a current density of >20 mA/cm^2.

[1] F. Sano et al., US-Japan Workshop on Negative Ion Based NBI Development, Berkeley, CA, Oct. 8–11, 1990.

[2] M. Bacal and G. W. Hamilton, Phys. Rev. Lett. **42** (1979) 1583.

[3] J. R. Hiskes and A. M. Karo, Appl. Phys. Lett. **54** (1989) 508.

[4] J. M. Wadehara, Phys. Rev. A **29** (1984) 106.

Fumimichi Sano
Plasma Physics Laboratory
Kyoto University
JAPAN

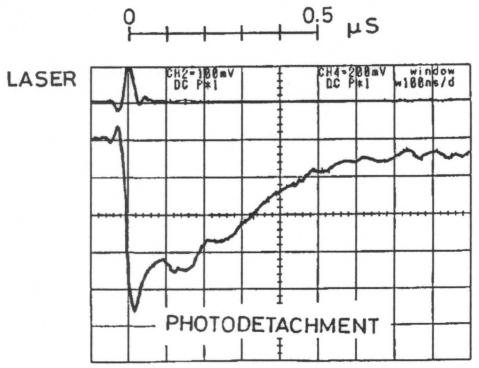

Fig. 2. Time evolution of the photodetachment signal in chamber II. A typical dacay time is on the order of 0.5 μs.

News from ATF

While the ATF is shut down for a transformer upgrade, data obtained during the last operation period have been analyzed. Transport and fluctuation data in the quadrupole field scan with neutral beam injection are of particular interest. In this scan, the quadrupole field was varied in the same way as in the bootstrap current studies with the vacuum magnetic axis $R_0^{(vac)}$ fixed at 2.08 m (with $\bar{n}_e = 5.3 \times 10^{19} m^{-3}$ and $P_{NBI} = 0.8$ MW). Figure 1(a) shows variations of the central and volume-average beta, $\beta(0)$ and $\langle\beta\rangle$, calculated from the profile analysis. The lengths of the bars representing $\beta(0)$ indicate fast-ion contributions to $\beta(0)$. The global energy confinement time $\tau_E^* = W_{dia}/P_{abs}$) based on the estimated absorbed power P_{abs} is equal to the kinetic gross energy confinement time, $\tau_E(a) = (W_e + W_i)/(P_{be} + P_{bi})$, based on calculated beam power transfer to electrons (P_{be}) and ions (P_{bi}) from the profile analysis. The

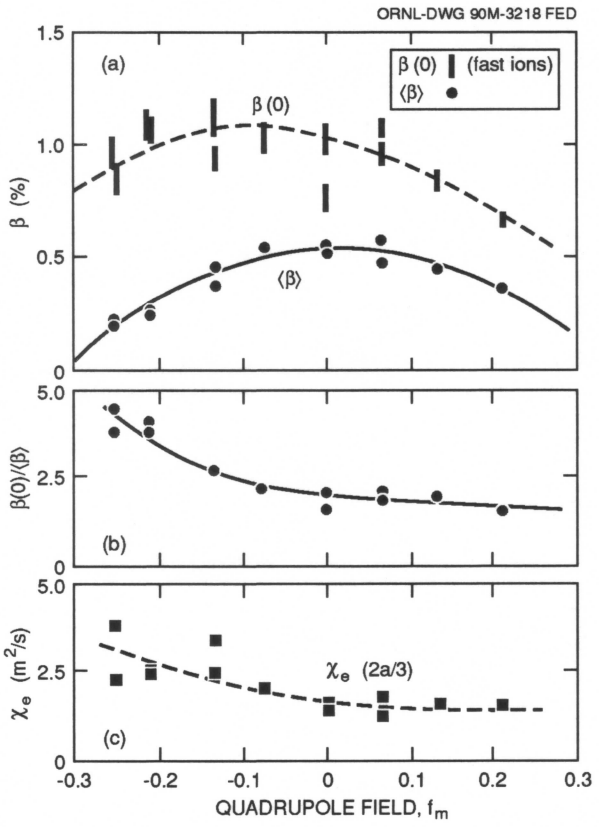

FIG. 1. Response of plasma parameters to the quadrupole field scan with NBI (R_0^{vac} = 2.08 m and B_0 = 0.95 T): (a) central and volume-average beta, (b) ratio of central to volume-average beta, and (c) electron thermal diffusivity at r = 2a/3, as a function of the quadrupole field ratio.

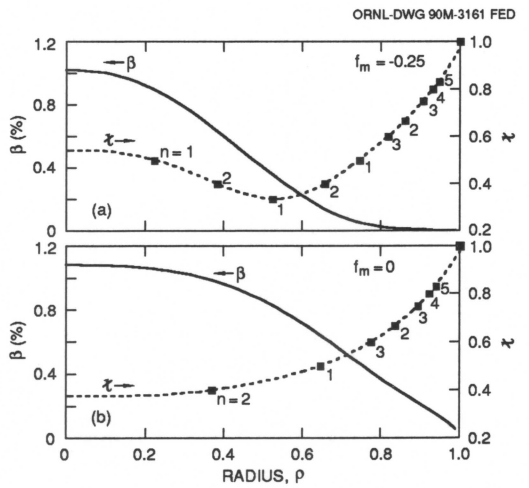

Fig. 2. Radial profiles of beta and rotational transform and resonance toroidal mode numbers for two cases in the NBI quadrupole scan: (a) narrow pressure profile case with f_m = 0.25 and (b) peaked pressure profile case with f_m = 0.

energy confinement times peak in the vicinity of the standard or slightly prolate configurations, as in the quadrupole scan with ECH alone. This trend is consistent with that of the thermal electron diffusivity derived from a local power balance [Fig. 1(c)]. The pressure profile shape is also affected by the quadrupole field variations. Figure 1(b) shows the ratio $\beta(0)/\langle\beta\rangle$ as a function of the quadrupole field. The pressure profiles become more peaked as the flux surfaces become more oblate. In spite of modest beta values with modest NBI power, the Shafranov shift is rather large ($\Delta_S/\bar{a}$ up to 0.25) for the oblate configuration. These variations of the pressure profiles and Shafranov shifts have significant effects on stability and fluctuations.

Figure 2(a) shows the effects of narrow pressure profiles on magnetic fluctuations with the quadrupole field ratio $f_m = -0.25$. The pressure profile is reminiscent of the profiles observed before the field error repair (but not as peaked). Double resonances at $\iota = 1/2$, 2/5, and 1/3 appear in the middle radial region ($0.2 < \rho < 0.8$) where the pressure gradient is at a maximum. The magnetic fluctuations observed with Mirnov coils show globally coherent modes with low toroidal mode numbers, $n = 1$ and 2. However, the central beta in these experiments was too low to reach the critical value above which the self-stabilization (second stability) dominates.

Effects of broad pressure profiles are represented by the $f_m = 0$ case [Fig. 2(b)] in the NBI quadrupole scan. The

broad pressure profile is typical of profiles obtained after the field error repair. There is no double resonance in $\iota(\rho)$, and the maximum pressure gradient appears near the plasma edge, where the resonances have higher n numbers. The observed fluctuations have higher n (n = 1–6) with short toroidal coherence lengths ($\Delta\varphi \approx$ one field period = 30°) Detailed studies of the harmonic spectra of $\tilde{B}$ signals in the operation period show that the rms fluctuation level of the coherent $\tilde{B}$ increases with increasing $\langle\beta\rangle$. At high beta, the $\tilde{B}$ signals are dominated by more toroidally localized disturbances at the edge of the plasma, where the local magnetic field curvature in the helical ripple wells is strongly destabilizing.

With the present broad pressure profiles, the beta values are still too low to show self-stabilization. Access to the second stability regime requires higher beta (with higher beam power) and/or more peaked profiles. A pressure profile control experiment with dynamic configuration variations using the quadrupole field would be an attractive way to access second stability in full bore ATF plasmas.

M. Murakami and J. H. Harris for the ATF Group
Oak Ridge National Laboratory
P.O. Box 2009
Oak Ridge, TN 37831-8072, USA

Visitors to the CHS Group

Dr. Larry Peranich (General Atomics, USA) stayed for seven weeks in October to participate in the experimental study of the effect of the error field on the confinement, which is discussed in "News from CHS" above.

Dr. Shinji Hiroe (Oak Ridge National Laboratory, USA) visited CHS in November and discussed radiation losses in ECH and NBI plasmas.

Determination of LHD Machine Configuration

Design Work History

The Large Helical Device (LHD) project is a major fusion research program under the Ministry of Education, Science and Culture. In 1986, the Nuclear Fusion Subcommittee of the Science Council recommended that a large helical device should be build in Toki City, Gifu Prefecture. Responding to this recommendation, the LHD design group was organized. In fiscal year (FY)1986, the LHD objectives were clarified and the l = 2 Heliotron/Torsatron-type continuous-coil configuration was adopted (see the Green LHD Design Book). Superconducting coil systems with m (helical pitch number) of 10–14 were studied in FY 1987 (see the Blue Design Book), and the standard magnetic configurations was selected as m = 10, γ (helical pitch parameter) ~1.2 in FY 1988 (see the Orange Design Book). After the foundation of the National Institute for Fusion Science (May 29,1989), a final machine configuration was chosen under the LHD Design Group.

Choice of Magnetic Configuration

Through several-years of design work, the optimal value of m was found to be near 10 for the LHD system with respect to compatibility among several physics and engineering requirements. The final magnetic configuration for LHD has been mainly determined by the following physics requirements within the related engineering constraints;

- High beta achievement ($\beta \geq 5\%$).
- Good confinement of energetic particles (loss-cone-free radius ($r_L \geq a_p/3$) for 70% ICRF heating efficiency).
- Divertor-wall clearance ($\Delta_{dw} \geq$ 3 cm).
- Maximization of transport properties.

The beta limit and the divertor condition require the m $\leq$10 for a medium-γ_c configuration ($\gamma_c = ma_c/lR \sim 1.2$–1.3). A higher-$\gamma_c$ configuration ($\gamma_c \geq 1.3$) cannot provide the divertor-wall clearance for 4-m/4-T LHD designs with an allowable coil current density of ~ 50 A/mm^2. In LHD a slight positive pitch modulation of the helical windings ($a_c = 0.1$, $\theta = (l/m)\,\varphi + a_c \sin(l\,\varphi/m)$) is found

to improve physics-engineering compatibility. A negative pitch modulation improves orbit confinement for small inward axis shift; however, the positive pitch modulation leads to more improvement for large inward shift.

As design candidates, we chose three systems,

(A) $m=10$, $\gamma_c=1.20$, $a_c=0.0$,
(B) $m=10$, $\gamma_c=1.20$, $a_c=0.1$,
(C) $m=10$, $\gamma_c=1.25$, $a_c=0.1$,

and compared their magnetic confinement properties of these three designs as a function of inward shift Δ_{ax}. For the (B) design, the compatibility between beta and orbit criteria is not satisfied. In the (A) and (C) designs, three conditions are matched at $\Delta_{ax} \sim -12.5$ cm and $\Delta_{ax} \sim -15$ cm, respectively.

Table 1. Specifications of LHD

Parameter	Phase I	Phase II
l	2	2
m	10	10
γ_c (pitch parameter)	1.25	1.25
a_c (pitch modulation)	0.1	0.1
Major Radius	3.9 m	3.3 m
Plasma Minor Radius	0.6–0.65 m	0.6–0.65 m
Plasma Volume	30 m^3	30 m^3
Magnetic Field	3.0 T	4.0 T
Helical Coil		
Magnetomotive Force	5.85 MAT	7.80 MAT
Current Density	40 A/mm^2	53.3A/mm^2
Coil Temperature	4.2 K	1.8 K
Maximum Field	7.2 T	9.6 T
Poloidal Coil		
Outer Vertical	-4.3 MAT	-4.3 MAT
Inner Shaping	-4.4 MAT	-4.4 MAT
Inner Vertical	4.9 MAT	4.9 MAT
Divertor		
Baffle Plate		Installed
Plasma duration	10 s	10 s
Repetition time	5 min	5 min
Heating		
ECH	10 MW	10 MW
NBI	15 MW	20 MW
ICRF	3 MW	9 MW
Steady-State Power		3 MW

In addition to these three conditions, we checked the neoclassical and anomalous transport rates. Among the three design options the maximum $n\tau T$ value can be obtained in the (C) design. Moreover, the (C) configuration is better than (A) from the viewpoint of reducing poloidal coil currents.

The final magnetic configuration for LHD was determined to be the optimized configuration ($l=2$, $m=10$, $\gamma_c=1.25$, $a_c=0.1$).

Engineering Design and R&D Programs of LHD

The machine design was carried out to satisfy the above mentioned design configuration, and the final specification of the LHD system have been determined as shown in Table 1. The experimental program is divided into two phases. To promote the LHD construction, several research and development (R&D) programs are being carried out.

Schedule of LHD Project

The budget for the first year of the seven-year construction period was approved by the Japanese government in 1989. The construction of LHD will be completed in 1997.

LHD Design Group
National Institute for Fusion Science
Nagoya 464-01, Japan

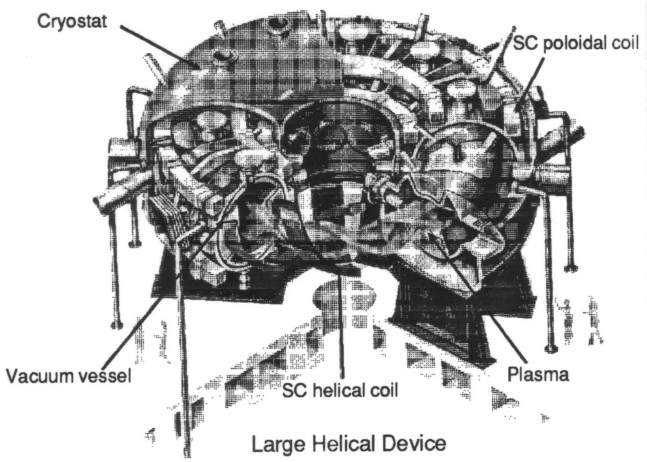

Large Helical Device